AIP | The Journal of Chemical Physics

Effect of cation species on surface-induced phase transition observed for platinum complex anions in platinum electrodeposition using nanoporous silicon

Ryo Koda, Akira Koyama, Kazuhiro Fukami, Naoya Nishi, Tetsuo Sakka, Takeshi Abe, Atsushi Kitada, Kuniaki Murase, and Masahiro Kinoshita

Citation: The Journal of Chemical Physics **141**, 074701 (2014); doi: 10.1063/1.4892596
View online: http://dx.doi.org/10.1063/1.4892596
View Table of Contents: http://scitation.aip.org/content/aip/journal/jcp/141/7?ver=pdfcov
Published by the AIP Publishing

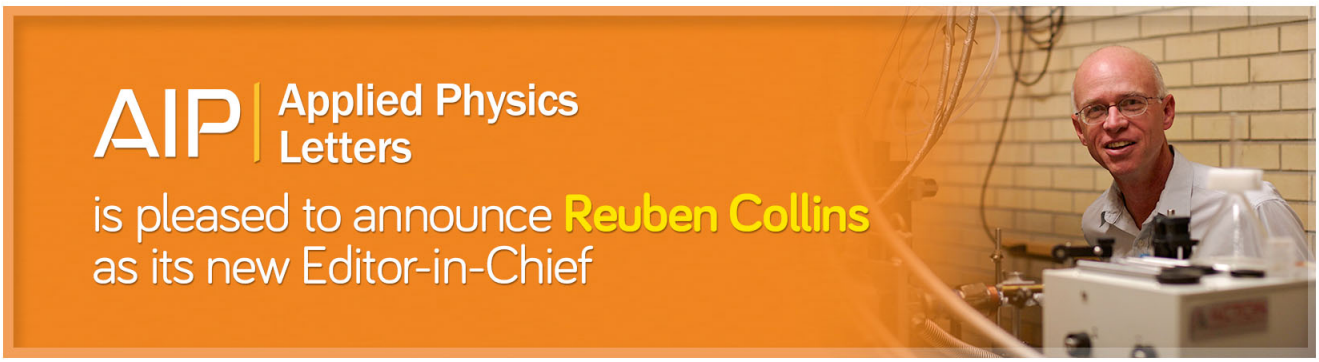

Effect of cation species on surface-induced phase transition observed for platinum complex anions in platinum electrodeposition using nanoporous silicon

Ryo Koda,[1] Akira Koyama,[2] Kazuhiro Fukami,[2,3,a)] Naoya Nishi,[1] Tetsuo Sakka,[1] Takeshi Abe,[1,3] Atsushi Kitada,[2] Kuniaki Murase,[2] and Masahiro Kinoshita[4,b)]
[1]*Department of Energy and Hydrocarbon Chemistry, Kyoto University, Kyoto 615-8510, Japan*
[2]*Department of Materials Science and Engineering, Kyoto University, Kyoto 606-8501, Japan*
[3]*Core Research for Evolution Science and Technology (CREST), Japan Science and Technology Agency (JST), Kawaguchi, Saitama 332-0012, Japan*
[4]*Institute of Advanced Energy, Kyoto University, Kyoto 611-0011, Japan*

(Received 3 July 2014; accepted 29 July 2014; published online 15 August 2014)

In an earlier work [K. Fukami *et al.*, J. Chem. Phys. **138**, 094702 (2013)], we reported a transition phenomenon observed for platinum complex anions in our platinum electrodeposition experiment using nanoporous silicon. The pore wall surface of the silicon electrode was made hydrophobic by covering it with organic molecules. The anions are only weakly hydrated due to their large size and excluded from the bulk aqueous solution to the hydrophobic surface. When the anion concentration in the bulk was gradually increased, at a threshold the deposition behavior exhibited a sudden change, leading to drastic acceleration of the electrochemical deposition. It was shown that this change originates from a surface-induced phase transition: The space within a nanopore is abruptly filled with the second phase in which the anion concentration is orders of magnitude higher than that in the bulk. Here we examine how the platinum electrodeposition behavior is affected by the cation species coexisting with the anions. We compare the experimental results obtained using three different cation species: K^+, $(CH_3)_4N^+$, and $(C_2H_5)_4N^+$. One of the cation species coexists with platinum complex anions $[PtCl_4]^{2-}$. It is shown that the threshold concentration, beyond which the electrochemical deposition within nanopores is drastically accelerated, is considerably dependent on the cation species. The threshold concentration becomes lower as the cation size increases. Our theoretical analysis suggests that not only the anions but also the cations are remarkably enriched in the second phase. The remarkable enrichment of the anions alone would give rise to the energetic instability due to electrostatic repulsive interactions among the anions. We argue that the result obtained cannot be elucidated by the prevailing view based on classical electrochemistry. It is necessitated to consult a statistical-mechanical theory of confined aqueous solutions using a molecular model for water. © *2014 AIP Publishing LLC*. [http://dx.doi.org/10.1063/1.4892596]

I. INTRODUCTION

Porous materials play imperative roles in the development of such devices as sensors, catalysts, fuel cells, rechargeable batteries, and capacitors.[1–7] In the utilization of porous structure for a reaction field, a larger specific surface area brought by decreasing the pore diameter and increasing the porosity can lead to higher performance of chemical or electrochemical reactions. To prepare porous structure with high performance, the pore size needs to be sufficiently small, i.e., of the scale of a few nanometers. In solution (i.e., solvent in which reactants are dissolved as solutes), however, the mass transfer of reactants within such nanopores is geometrically hindered, and the extent of the hindrance becomes prominent with a decrease in the pore diameter. This is particularly true for deep pores. As a salient example, an electrochemical reaction within nanopores is remarkably decelerated once a diffusion-limited condition is reached due to the difficulty in supply of reactants from the bulk.[8,9] Thus, it is often difficult in chemical or electrochemical reactions to elicit suitably high performance even when quite a large specific surface area is conferred to the porous structure. Design and control of injection into and ejection from nanopores is an important, challenging issue in modern nanotechnology.

Let us consider liquid or liquid mixture confined by a surface. The structure near the surface, which is referred to as "surface-induced structure," is substantially different from that in the bulk. This is evidenced in, for instance, recent studies on ionic liquids near solid surfaces by scanning probe microscopy, nuclear magnetic resonance, ellipsometry, and X-ray reflectometry.[10–14] Theoretical studies[15–18] have argued that the surface-induced structure is largely influenced by the surface-liquid affinity. The solute concentration near the surface can remarkably be different from that in the bulk. The details of the difference are determined by complex interplay of the solvent-solute, surface-solvent, and surface-solute affinities.[19–24] Liquid, liquid mixture, or solution confined

a)Electric mail: fukami.kazuhiro.2u@kyoto-u.ac.jp
b)Electric mail: kinoshit@iae.kyoto-u.ac.jp

between two surfaces, when the surface separation is sufficiently small, may exhibit the structure and properties which are entirely different from those in the bulk. When it is confined within a nanopore, its structure and properties can be diverse, depending upon the pore diameter and the solvent, solute, and pore wall surface characteristics.

In recent works,[25,26] we have investigated platinum electrodeposition within nanoporous silicon electrode (the pore diameter is ∼3 nm on the average). The electrode is immersed in aqueous solution containing platinum complex ions (these are anions). The pore wall surface of the electrode is made hydrophobic by covering it with organic molecules and platinum complex ions with sufficiently large sizes, $[PtCl_4]^{2-}$, are adopted. Such ions are only weakly hydrated and excluded from the bulk with the result that the ionic concentration is largely enriched near the hydrophobic surface: They are rather hydrophobic in this sense. When the ion concentration in the bulk is gradually increased, at a threshold the deposition behavior exhibits a sudden change, leading to drastic acceleration of the electrochemical deposition.[26] Using our statistical-mechanical theory for confined molecular liquids, we have shown that this change originates from a surface-induced phase transition: The space within a nanopore is abruptly filled with the second phase in which the ion concentration is orders of magnitude higher than that in the bulk.[26] The threshold concentration is lowered when the ionic size is made larger (that is, $[PtCl_4]^{2-}$ with $d_- = 0.60$ nm (d_- is the anion diameter) is replaced by $[PtBr_4]^{2-}$ with $d_- = 0.70$ nm; the latter is more hydrophobic).[25,26] When the pore wall surface is made hydrophilic, by contrast, there is no such striking behavior observed: It seems that the enrichment of the ionic concentration near the hydrophilic surface does not occur and the electrochemical deposition within nanopores does not proceed irrespective of the ionic concentration in the bulk. Near the hydrophilic surface, the concentration of the hydrophobic solute is not enriched but the number density of water is considerably heightened.

In the platinum electrodeposition experiment described above, we have been successful in producing platinum nanoparticles whose diameters are smaller than the pore diameter (∼3 nm).[26] Below the threshold concentration, only filmy deposition is achieved on the top surface of porous silicon with essentially no deposition within nanopores. Above the threshold concentration, the nanoparticles are always deposited within nanopores. The surface-induced phase transition is thus crucial in the production of nanoparticles. Another significant finding is that the packing fraction of the nanoparticles produced within a nanopore can readily be controlled by adjusting the size of platinum complex ions.[25,26] In the second phase filling nanopores, the ion concentration for $[PtBr_4]^{2-}$ is considerably higher than that for $[PtCl_4]^{2-}$, even when the ion concentrations in the bulk share the same value. Therefore, each nanopore is more densely packed with nanoparticles as the ion size is increased. It should be noted that this type of control is substantially different from the conventional one manipulating the applied potential, current density, or temperature of the electrochemical cell.

In the present study, we examine the effect of cations coexisting with $[PtCl_4]^{2-}$ on the platinum electrodeposition behavior. We compare the experimental results obtained using three different cation species: K^+, $(CH_3)_4N^+$, and $(C_2H_5)_4N^+$. It is shown that the threshold concentration, beyond which the electrochemical deposition within nanopores is drastically accelerated, is considerably dependent on the cation species which coexists with platinum complex anions. It follows that the cation species and its concentration in the bulk are also useful manipulated variables for controlling the deposition behavior. These results, which can hardly be expected from the standpoint of classical electrochemistry, are analyzed using our statistical-mechanical theory combined with a molecular model for water. The conclusion thus drawn is the following: The surface-induced phase transition for an anion species with a large size is substantially influenced by a coexisting cation species with a large size; and the influence becomes stronger as the cation size increases.

II. MATERIALS AND METHODS

Silicon wafers were purchased from Shin-Etsu Astech Co., Ltd., and all the chemicals were purchased from Nacalai Tesque, Inc. with analytical grade. Porous silicon electrodes were prepared by anodization of p-type silicon (100) with a resistivity in the range 3–5 Ω cm. The anodization was carried out in 22 wt. % HF solution (48 wt. % HF: ethanol = 1: 1.7 in volume) at 2.0 mA cm^{-2} for 20 min. The average diameter of the pores was about ∼3 nm (the maximum diameter was ∼5 nm), and the thickness of porous layer was 1 μm.

Displacement deposition of platinum (see Sec. III A) was performed using the porous silicon as the working electrode. Platinum complex (K_2PtCl_4) and one of the three salts, potassium chloride (KCl), tetramethylammonium chloride ($(CH_3)_4NCl$), and tetraethylammonium chloride ($(C_2H_5)_4NCl$), were added to ultra pure water (Millipore Reference A^+, the resistivity of water was 18.2 MΩ cm). Each of the resultant solutions was used for the platinum deposition bath: K^+, $(CH_3)_4N^+$, or $(C_2H_5)_4N^+$ coexisted with $[PtCl_4]^{2-}$ in the solution. The concentration of KCl, $(CH_3)_4NCl$, or $(C_2H_5)_4NCl$ (i.e., that of K^+, $(CH_3)_4N^+$, or $(C_2H_5)_4N^+$) in the bulk was fixed at 0.5 M and that of K_2PtCl_4 (i.e., that of $[PtCl_4]^{2-}$) in the bulk was changed from 0.006 M to 0.010 M with the increment of 0.001 M. Thus, we looked at the deposition behavior for the 15 different solutions. In all the experiments, the displacement deposition was carried out for 2 h. As described in Sec. III A, the open circuit potential was measured after a porous silicon electrode was simply immersed in the deposition bath.

The cross-sectional views of the microporous silicon electrode after platinum displacement deposition were observed by a field-emission type scanning electron microscope (JEOL, JSM-6500F; SEM).

III. EXPERIMENTAL RESULTS AND DISCUSSION

A. Concept of displacement deposition in porous silicon

In our earlier works,[25,26] the surface of porous silicon was made hydrophobic by covering it with organic molecules. For

the as-prepared porous silicon used in the present study, such treatment is not necessary because its surface is terminated by Si–H bonds and inherently hydrophobic. The as-prepared porous silicon can spontaneously be oxidized in aqueous solution containing $[PtCl_4]^{2-}$. This spontaneous oxidation occurs together with the deposition of platinum on the silicon surface. Such deposition is categorized as *displacement deposition*.[27] The redox reactions can be written as follows: $[PtCl_4]^{2-} + 2e^- \rightarrow Pt + 4Cl^-$ and $Si + 2H_2O + 4h^+ \rightarrow SiO_2 + 4H^+$. Under the condition where a nanopore is filled with the second phase due to the surface-induced phase transition, the displacement deposition occurs drastically on the porous silicon wall, and platinum nanoparticles whose diameters are determined by the nanopore diameter are spontaneously produced without an external bias. Platinum is deposited within nanopores by this displacement deposition scheme in our experiment of the present study.

The oxidation of silicon during the displacement deposition should lead to only a slight change in the surface hydrophobicity. This is because the oxidation of silicon starts not from that of "Si–H" to "Si–OH" but from the backbond oxidation yielding "Si–O–Si":[28] Most of the Si–H bonds still remain on the surface, leading to the persistence of the surface hydrophobicity during our deposition experiment.

B. Effect of coexisting cations on displacement deposition of platinum in porous silicon

Figure 1 shows cross-sectional SEM images of nanoporous silicon after the displacement deposition of platinum under a prescribed concentration of $[PtCl_4]^{2-}$ in the bulk with the three species of coexisting cations. At $C = 0.006$ M (C is the concentration of $[PtCl_4]^{2-}$ in the bulk), the deposition does not proceed at all within the nanoporous layer in all the K^+, $(CH_3)_4N^+$, and $(C_2H_5)_4N^+$ solutions as observed in Figs. 1(a)–1(c). At $C = 0.007$ M (Figs. 1(d)–1(f)), platinum is successfully deposited within nanopores only in $(C_2H_5)_4N^+$ solution. At $C = 0.008$ M (Figs. 1(g)–1(i)) and 0.009 M (Figs. 1(j)–1(l)), the platinum deposition is achieved within the nanoporous layer in $(CH_3)_4N^+$ and $(C_2H_5)_4N^+$ solutions but not in K^+ solution. At $C = 0.010$ M (Figs. 1(m)–1(o)), the platinum deposition is successful in all the K^+, $(CH_3)_4N^+$, and $(C_2H_5)_4N^+$ solutions.

Taken together, the platinum deposition in nanoporous silicon is suddenly accelerated at a threshold concentration C^{ex} in each of the three different solutions. The values of C^{ex} for K^+, $(CH_3)_4N^+$, and $(C_2H_5)_4N^+$ solutions are, respectively, in the rages 0.009−0.010 M, 0.007−0.008 M, and 0.006−0.007 M. The threshold concentration is dependent upon the cation species which coexists with $[PtCl_4]^{2-}$.

C. Electrochemical behavior in platinum deposition analyzed using prevailing view

We measured the relation between current density and electrode potential for a flat silicon electrode, that is, the so-called *i-E* curve. The measurement serves as one of the typical methods to evaluate the electrochemical behavior. Figure 2 shows *i-E* curves measured for the flat silicon electrode in K^+, $(CH_3)_4N^+$, and $(C_2H_5)_4N^+$ solutions containing $[PtCl_4]^{2-}$ at $C = 0.008$ M. We emphasize that the experiment described in Sec. II was performed not for a flat surface but for nanopores. In Fig. 2, all the curves are essentially

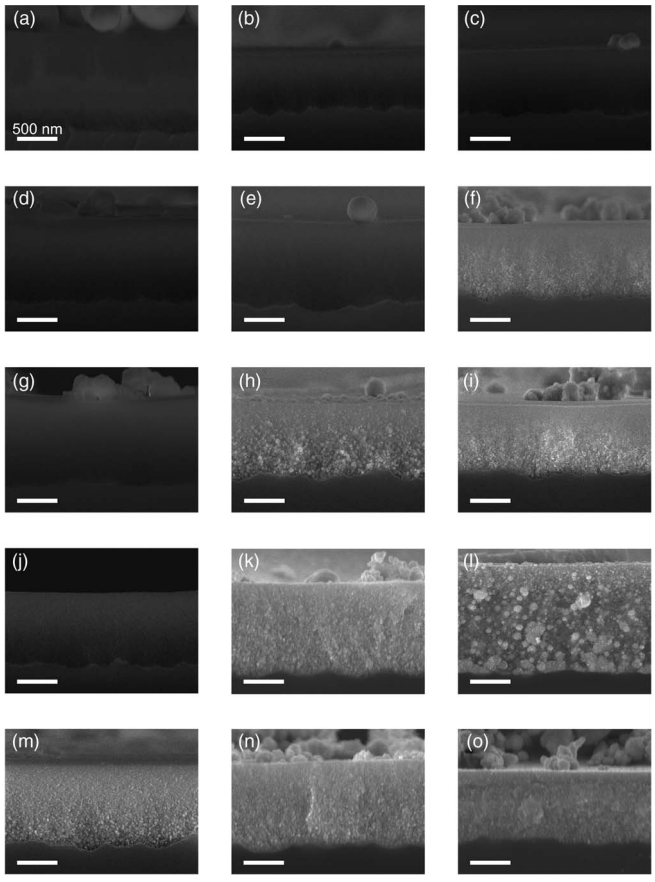

FIG. 1. Cross-sectional SEM images of porous silicon after platinum displacement deposition. Samples on the left column (a, d, g, j, and m), middle column (b, e, h, k, and n), and right column (c, f, i, l, and o) were prepared, respectively, in 0.5 M of KCl, $(CH_3)_4NCl$, and $(C_2H_5)_4NCl$ solutions containing $[PtCl_4]^{2-}$ at the five different concentrations: 0.006 M (a, b, and c), 0.007 M (d, e, and f), 0.008 M (g, h, and i), 0.009 M (j, k, and l), and 0.010 M (m, n, and o). The scale bar indicates 500 nm.

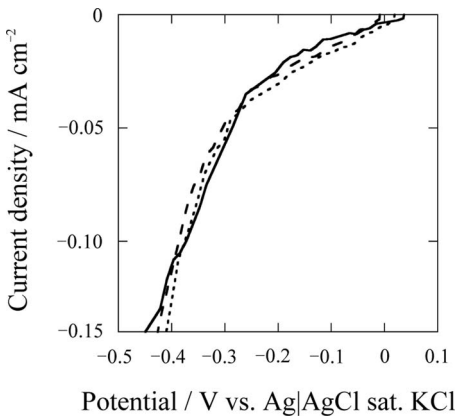

FIG. 2. Current density versus potential curves measured for a flat silicon electrode in aqueous solutions containing 0.5 M of KCl (solid line), $(CH_3)_4NCl$ (dotted line), and $(C_2H_5)_4NCl$ (dashed line). The concentration of $[PtCl_4]^{2-}$ was 0.008 M. Scan rate was 10 mV/s. Although all the curves are almost perfectly overlapped, the platinum deposition within nanopores behaved quite differently (see Figs. 1(g)–1(i)).

indistinguishable, implying that the electrochemical behavior remains almost the same, being independent of the species of coexisting cations. This result indicates that the partial-wetting transition (see Sec. IV A) does not occur for a *flat surface* at $C = 0.008$ M in the aqueous solution employed in our experiment. The sudden acceleration of platinum deposition within nanopores at a threshold concentration of $[PtCl_4]^{2-}$ (Fig. 1), which manifests a transition phenomenon, should originate not from the electrochemical behavior but from the surface-induced phase transition.

The reaction rate of platinum displacement deposition is defined using the electrode potential where the reduction of platinum and the oxidation of silicon are balanced with each other. In other words, the net electric current flowing through the external circuit is zero. The current for the platinum deposition can be expressed by the equation,

$$I_{Pt} = nFAC_{[PtCl4]2-}k(\phi), \tag{1}$$

where I_{Pt} denotes the current arising from the reduction of platinum that is balanced with the oxidation of silicon, n the number of electrons per a platinum complex ion reduced, F the Faradaic constant, A the surface area, $C_{[PtCl4]2-}$ the $[PtCl_4]^{2-}$ concentration at the surface, and $k(\phi)$ the reaction rate constant which is a function of the electrode potential ϕ. The diameters and depths of nanopores in silicon should remain unchanged during our experiment. This means that A as well as n and F is a constant. According to the result shown in Fig. 2, the current is independent of the cation species coexisting with $[PtCl_4]^{2-}$. A flat (non-porous) silicon electrode was employed in the *i-E* curve measurement. The electrochemical reaction took place on a single surface for which the partial-wetting transition could not occur as described above. The concentration of the platinum complex anions at the surface is not significantly influenced by the cation species with the result that $k(\phi)$ is not, either. It follows that I_{Pt} is dependent upon $C_{[PtCl4]2-}$ alone. Thus, the prevailing view based on classical electrochemistry applied to a flat electrode is incapable of elucidating the essential effect of the cation species.

As described above and in our earlier publications,[25,26] the behavior of platinum deposition within nanopores in porous silicon is strongly influenced by the surface-water affinity (i.e., hydrophobicity or hydrophilicity of the pore wall surface), size of platinum complex anions (i.e., $[PtCl_4]^{2-}$ or $[PtBr_4]^{2-}$; even when the ionic strength is the same), and cation species coexisting with the anions in the aqueous solution. Moreover, the deposition behavior does not change monotonically as the anion concentration in the bulk increases: It exhibits a sort of transition phenomenon. Elucidation of this sophisticated result is made possible only by consulting a liquid-state theory based on statistical mechanics. In what follows, we review the surface-induced phase transition phenomena for solutions confined by a single surface or two surfaces and for solutions constrained within a nanopore. Model analysis which is closely related to the phenomena observed in the present experiment is also implemented.

IV. THEORETICAL ANALYSIS

A. Concept of surface-induced phase transition

The concept of the surface-induced phase transition has been developed by Kinoshita[19–24,29] using some different versions of the integral equation theory (IET). The surface-induced phase transition is most likely to occur for water containing a low concentration of hydrophobic solute near a hydrophobic surface or for nonpolar liquid containing a low concentration of hydrophilic solute near a hydrophilic surface. In the former, the hydrophobic solute, which cannot participate in the hydrogen bonding of water, is excluded from water and its concentration is enriched near the hydrophobic surface. In the latter, the hydrophilic solute, which feels quite uncomfortable in nonpolar liquid, preferentially comes to the hydrophilic surface with the result of the enrichment of its concentration.

As the solute concentration in the bulk C increases, the enrichment mentioned above becomes stronger, whereas the thickness of the enriched layer is microscopic in the sense that it is comparable with the solute size. However, near a threshold value of C, C^*, the Fourier transform of the surface-solute total correlation function at zero wave vector exhibits an abrupt increase toward infinity, which indicates that the surface-solute correlation becomes quite intense and long ranged. This can be identified as a signal of a transition phenomenon exhibiting a sudden growth of the enriched layer: The thickness of the layer grows from a microscopic scale to a submacroscopic one, and the solute concentration within the layer becomes much higher. We note that the thickness is not of a macroscopic scale because the bulk is thermodynamically stable as a single phase. The transition is referred to as the *partial-wetting transition* representing the partial wetting of the surface by the solute.[19,20,24,29] C^* is the spinodal point beyond which the microscopic surface-induced layer becomes unstable. Beyond C^* the IET possesses no solutions. In the real system, the transition occurs at the concentration that is lower than C^*, C^+ ($C^+ < C < C^*$ is the region which is metastable for the microscopic surface-induced layer). Let the thickness of the surface-induced layer be δ. The average solute concentration in the layer and δ should be increasing functions of $C > C^*$ though they cannot be calculated by the IET.

We then consider the solution confined between two surfaces (e.g., water containing a low concentration of hydrophobic component (i.e., solute) confined between two hydrophobic surfaces) with the surface separation L that is sufficiently small. When the solute concentration in the bulk C is gradually increased, the confined domain is unavoidably filled with the second phase (e.g., hydrophobic component containing a low concentration of water) beyond a threshold value of C, C^{**}, which is referred to as the *bridging transition* implying that the two enriched layers bridge each other.[21–24] In the case of $L \sim 2\delta$, the spinodal point of the bridging transition C^{**} is approximately equal to C^*: $C^{**} \sim C^*$. For $L < 2\delta$, however, it is lower than C^* for a single surface ($C^{**} < C^*$); it becomes lower as L decreases; and for very small L, the transition occurs at a remarkably low solute concentration in the bulk. Actually, the transition occurs at $C = C^{++}$ ($C^{++} < C^{**}$,

$C^{++} \leq C^{+}$). Beyond C^{**}, the system without the second phase cannot exist even as the metastable state. $C^{++} < C < C^{**}$ is the region which is metastable for the system without the second phase. As for the liquid confined within a nanopore with diameter d_P, its behavior is more influenced by the surface properties than the behavior of the liquid confined between two surfaces with the surface separation $L = d_P$. The region which is metastable for the system without the second phase is represented by $C^{+++} < C < C^{***}$ (C^{***} is the spinodal concentration, the actual transition occurs at $C = C^{+++}$, $C^{***} < C^{**}$, and $C^{+++} < C^{++}$). Further, the influence becomes larger as d_P decreases. The transition, upon which the pore is unavoidably filled with the second phase, occurs at a lower solute concentration in the bulk for smaller d_P. In the present article, the transition occurring within a nanopore is also referred to as the bridging transition.

The two types of surface-induced phase transitions, partial-wetting and bridging transitions, occur even when the bulk is quite stable as a single phase. The existence of these transitions has been reproduced by computer-simulation and experimental studies. By using Grand Canonical Monte Carlo simulations, Greberg and Patey[30] verified the occurrence of the bridging transition for model systems mimicking water containing a low concentration of hydrophobic solute confined between hydrophobic surfaces and nonpolar liquid containing a low concentration of water confined between hydrophilic surfaces. Kurihara and co-workers[31] experimentally studied cyclohexane-ethanol binary liquid near a single silica (SiO_2) surface. Their system corresponds to nonpolar liquid (cyclohexane) containing a low concentration of hydrophilic solute (ethanol) near a hydrophilic surface (silica surface). They gradually increased the ethanol concentration from zero: They observed an abrupt formation of an ethanol layer whose thickness reached ~15 nm at the ethanol concentration of ~0.1 mol. %. This manifests the existence of the partial-wetting transition.

We have recently demonstrated the existence of the bridging transition for the aqueous electrolyte solution, water containing K_2PtCl_4 or K_2PtBr_4, confined within a pore with a scale of a few nanometers.[26] The pore surface is made hydrophobic. The platinum complex anions, $[PtCl_4]^{2-}$ and $[PtBr_4]^{2-}$, behave as rather hydrophobic solutes due to their large sizes. As the anion size becomes larger with its charge kept constant, hydrogen atoms in water molecules with positive partial charges cannot come closer to it, leading to weaker stabilization by the electrostatic attractive interaction. That is, a sufficiently large anion possesses only weak affinity with water. We have shown the following: When the anion concentration in the bulk is gradually increased, at a threshold the space within a nanopore is abruptly filled with the second phase in which the anion concentration is remarkably higher than in the bulk. The threshold concentration for $[PtBr_4]^{2-}$ is lower than that for $[PtCl_4]^{2-}$.

B. Angle-dependent integral equation theory for molecular liquid near a surface

It is crucial to adopt a molecular model for water in the investigation of the ion-size effects. A water molecule is modeled as a hard sphere with diameter $d_S = 0.28$ nm in which a point dipole and a point quadrupole of tetrahedral symmetry are embedded.[32,33] The influence of molecular polarizability of water is included by employing the self-consistent mean field (SCMF) theory.[32,33] At the SCMF level the many-body induced interactions are reduced to pairwise additive potentials involving an effective dipole moment. Hard spherical cations and anions with diameters d_+ and d_-, respectively, are immersed in our model water. The water-water and water-ion correlations are then dependent not only on the distance between centers of the particles but also on the orientations of water molecules. We analyze the structure of aqueous electrolyte solution at an extended, uncharged (hydrophobic) surface. The water-surface correlations are also dependent on the orientations of water molecules.

We employ the angle-dependent integral equation theory (ADIET),[29,32–49] a statistical-mechanical theory for molecular liquids. A large, spherical particle (neutral hard sphere) with diameter $d_L = 30d_S$ mimicking an extended hydrophobic surface is immersed in our model aqueous electrolyte solution. The subscripts, "S," "+," "−," and "L," respectively, represent "solvent (water)," "cations," "anions," and "large particle." The Ornstein-Zernike (OZ) equation for the mixture comprising the large particle, water molecules, cations, and anions can be written as[29,32–49]

$$\eta_{\alpha\beta}(12) = \{1/(8\pi^2)\}\sum_{\gamma}\rho_{\gamma}\int c_{\alpha\gamma}(13)\{\eta_{\gamma\beta}(32) + c_{\gamma\beta}(32)\}d(3), \tag{2a}$$

$$\eta_{\alpha\beta}(12) = h_{\alpha\beta}(12) - c_{\alpha\beta}(12); \quad \alpha, \beta = \mathrm{S}, +, -, \mathrm{L}, \tag{2b}$$

where h and c are the total and direct correlation functions, respectively, (ij) represents $(\boldsymbol{r}_{ij}, \boldsymbol{\Omega}_i, \boldsymbol{\Omega}_j)$, $\boldsymbol{r}_{ij}$ is the vector connecting the centers of particles i and j, $\boldsymbol{\Omega}_i$ denotes the three Euler angles describing the orientation of particle i, $\int d(3)$ represents integration over all position and angular coordinates of particle 3, and ρ is the number density. The closure equation is expressed by[29,32–49]

$$c_{\alpha\beta}(12) = \int_{r_{12}}^{\infty}[h_{\alpha\beta}(12)\partial\{w_{\alpha\beta}(12) - b_{\alpha\beta}(12)\}/\partial r'_{12}]dr'_{12} - u_{\alpha\beta}(12)/(k_{\mathrm{B}}T) + b_{\alpha\beta}(12), \tag{3a}$$

$$w_{\alpha\beta}(12) = -\eta_{\alpha\beta}(12) + u_{\alpha\beta}(12)/(k_{\mathrm{B}}T), \tag{3b}$$

where u is the pair potential, b is the bridge function, and $r_{12} = |\boldsymbol{r}_{12}|$. In the present analysis, the hypernetted-chain (HNC) approximation is employed ($b = 0$). We assume that the macroparticle is present at infinite dilution ($\rho_L \to 0$). The calculation process can then be split into two steps:

Step (i). Solve Eqs. (2) and (3) for bulk aqueous electrolyte solution. Calculate the correlation functions X_{SS}, X_{S+}, X_{S-}, X_{++}, X_{+-}, and X_{--} ($X = h, c$).

Step (ii). Solve Eqs. (2) and (3) for the macroparticle-aqueous electrolyte solution system using the correlation functions obtained in step (i) as input data. Calculate the correlation functions X_{LS}, X_{L+}, and X_{L-} ($X = h, c$).

For the numerical solution of Eqs. (2) and (3), the pair potentials and correlation functions are expanded in a basis set of rotational invariants (i.e., Wigner's generalized spherical harmonics), and the basic equations are reformulated in terms of the projections $X_{\alpha\beta}{}^{mnl}{}_{\mu\nu}(r)$ (r is the distance between centers of two particles) occurring in the rotational-invariant expansion of $X_{\alpha\beta}(12)$. The expansion considered for $m, n \leq n_{\max} = 4$ gives sufficiently accurate results. The basic equations are then numerically solved using the robust, highly efficient algorithm developed by Kinoshita and coworkers.[38,40] In the numerical treatment, a sufficiently long range r_L is divided into N grid points ($r_i = i\delta r$, $i = 0, 1, \ldots, N-1$; $\delta r = r_L/N$) and all of the projections are represented by their values on these points. The grid width and the number of grid points are set at $\delta r = 0.01 d_S$ and $N = 4096$, respectively. The versatility and reliability of the ADIET was demonstrated in our earlier works on a variety of subjects (more details were described in our last publication[26] treating the electrochemical deposition of platinum within nanoporous silicon).

In the real system treated in the present study, the solution is confined within pores having various sizes whose surfaces are concave. However, the analysis on the solution confined by an extended surface and the partial-wetting transition provides fundamental information which can readily be applied to the solution confined between two extended surfaces and the solution within a nanopore in a semi-quantitative sense (see Sec. IV A). The microstructure (heterogeneity) of the surface is not taken into account in the theoretical calculation. However, it has been shown that it has no essential effects on the conclusion as long as the *averaged* properties of the surface-induced structure are discussed.[50]

C. Model aqueous electrolyte solution considered

$[PtCl_4]^{2-}$ is considered as the platinum complex anion. Following our last publication[26] treating the electrochemical deposition of platinum within nanoporous silicon, we model $[PtCl_4]^{2-}$ as a hard sphere within which the point charge of $-2e$ (e is the elementary electric charge) is placed at its center. The size of $[PtCl_4]^{2-}$ is approximately calculated from the molecular weight and density of K_2PtCl_4 in solid state with the tetragonal crystal structure: We obtain $d_-/d_S = 2.16$. As described in Sec. IV B, only a single salt species can be treated in our computer program based on the ADIET. We therefore consider water containing X_2PtCl_4 whose concentration in the bulk is C. The cation X^+ is modeled as a hard sphere within which the point charge of e is placed at its center. The diameter of $(CH_3)_4N^+$ is roughly estimated from the molecular weight and density of $(CH_3)_4NCl$ in solid state by assuming that it possesses the close-packed structure and $(CH_3)_4N^+$ is spherical: The result is $d_+/d_S \sim 2$. We note that $(C_2H_5)_4N^+$ is larger than $(CH_3)_4N^+$. In our theoretical analysis, the three different values of d_+ are tested: $d_+/d_S = 1.08$, 1.80, and 2.00. $d_+/d_S = 1.08$ corresponds to the value for K^+.[26] Though $d_+/d_S = 1.80$ and 2.0 do not strictly correspond to $(CH_3)_4N^+$ or $(C_2H_5)_4N^+$, they are useful in examining the effect of the size of coexisting cations d_+. A cation and an anion carry the charges e and $-2e$, respectively, and $\rho_+ = 2\rho_-$.

In our last publication mentioned above,[26] we analyzed water containing K_2PtCl_4 near a hydrophobic surface and found the occurrence of the partial-wetting transition in which the hydrophobic solute is $[PtCl_4]^{2-}$. In the present study, we consider X_2PtCl_4 ($d_+/d_S = 1.08$, 1.80, and 2.00) to know how the spinodal concentration C^* is affected by the size of X^+, d_+. When the concentration of X_2PtCl_4, C, is given, ρ_+ and ρ_- are automatically determined. Since C is very low, ρ_S is fixed at the pure-water value.

D. Aqueous electrolyte solution near a hydrophobic surface: A surface-induced layer

We restate that all the calculations are performed for uncharged surfaces. The concentration profile of cations or anions is described by $g_{Lj}(\xi) = h_{Lj}(\xi) + 1 = \rho_{Lj}(\xi)/\rho_j$ ($j = +, -$) where ξ is the distance from the surface in the surface-normal direction, $\rho_{Lj}(\xi)$ is the number-density profile of cations or anions, and ρ_j is the number density of cations or anions in the bulk ($g_{Lj}(\xi) \to 1$ as $\xi \to \infty$). Even when C is much lower than the spinodal concentration, ions with large sizes are largely enriched near the hydrophobic surface. The degree of the enrichment follows the order: X^+ with $d_+/d_S = 2.00 > X^+$ with $d_+/d_S = 1.80 > [PtCl_4]^{2-}$. These ions, which behave as rather hydrophobic solutes, are often referred to as "ions exhibiting negative hydration." For more information, in the case of $C = 0.00605$ M, $g_{L-}(0) = 29.99$ for $[PtCl_4]^{2-}$ and $g_{L+}(0) = 166.4$ for X^+ with $d_+/d_S = 1.80$; in the case of $C = 0.00189$ M, $g_{L-}(0) = 39.61$ for $[PtCl_4]^{2-}$ and $g_{L+}(0) = 656.0$ for X^+ with $d_+/d_S = 2.00$. The strong enrichment of the ion concentration occurs only in the vicinity of the surface. $g_{Lj}(\xi)$ reduces quite rapidly as ξ increases (a more detailed discussion on $g_{Lj}(\xi)$ is given in Sec. IV F). In this sense, the layer within which the ion concentration is enriched is microscopic. On the other hand, ions with small sizes are preferentially hydrated in the bulk, with the result that they are depleted near the hydrophobic surface. These ions, which behave as highly hydrophilic solutes, are often referred to as "ions exhibiting positive hydration." X^+ with $d_+/d_S = 1.08$, K^+, and Cl^- (with $d_-/d_S = 1.16$) belong to these ions.

Our experience in analyses on confined aqueous electrolyte solutions has shown the following. Let us consider the solution confined between two extended surfaces. When the surface separation L is not small, the solution around the center within the confined space is very much like that in the bulk and the normalized number-density profile of ions near each of the surfaces is close to that near a single surface. As L becomes smaller, the solution for all ξ is more influenced not only by the nearest surface but also by the other surface. For ions with large sizes, for example, when L becomes smaller than a few times of the diameter of a water molecule, the normalized number-density profile for all ξ exhibits an upward shift and the ion-size effect becomes larger. As discussed in our recent publication,[26] the upward shift and the enhancement of ion-size effect are more appreciable when L is smaller or the surface is concave and its curvature is larger. By the interplay of these physical factors, the enrichment of ion concentration and the ion-size effect becomes even larger when

the solution is confined within a pore having the size of a nanometer.

E. Analysis on partial-wetting transition

In order to investigate the partial-wetting transition[19,20,24,29] in the present system, we monitor the two quantities, $H_{\mathrm{L}j}(0)$ $(j = +, -)$. $H_{\mathrm{L}j}(k)$ is the Fourier transform of $h_{\mathrm{L}j}(r)$:

$$H_{\mathrm{L}j}(k) = 4\pi \int_0^\infty r^2 h_{\mathrm{L}j}(r)\{\sin(kr)/(kr)\}dr. \tag{4a}$$

$H_{\mathrm{L}j}(0)$ expressed by

$$H_{\mathrm{L}j}(0) = 4\pi \int_0^\infty r^2 h_{\mathrm{L}j}(r)dr \tag{4b}$$

gives a signal of the transition phenomenon as described above. Divergence of $H_{\mathrm{L}j}(0)$ at the spinodal concentration C^* implies that the surface-cation or surface-anion correlation becomes quite intense and long ranged (i.e., not of a microscopic scale).

F. Partial-wetting transition: Effect of cation size

The theoretical analysis is made for the partial-wetting transition near a single, extended hydrophobic surface. For $d_+/d_{\mathrm{S}} = 1.08$, Fig. 3(a) or 3(b) shows the plot of $H_{\mathrm{L}+}(0)$ or $H_{\mathrm{L}-}(0)$ against the concentration of $[PtCl_4]^{2-}$ in the bulk denoted by C. It is found that $H_{\mathrm{L}+}(0)$ and $H_{\mathrm{L}-}(0)$ simultaneously exhibit the divergent behavior at the spinodal concentration C^*. This is true even for $d_+/d_{\mathrm{S}} = 1.08$. As observed in the figure, they tend to diverge at $C^* \sim 0.0254$ M. This behavior is a signal of the partial-wetting transition, a sudden growth of the enriched layer from a microscopic scale to a submicroscopic one. C^* is the spinodal point (the spinodal concentration) explained above. The divergence of $H_{\mathrm{L}-}(0)$ is followed by that of $H_{\mathrm{L}+}(0)$. As C approaches C^*, the normalized density profiles of cations and anions in the vicinity of the surface ($g_{\mathrm{L}+}(\xi)$ and $g_{\mathrm{L}-}(\xi)$, respectively; ξ is the distance from the surface in the surface-normal direction) make the changes illustrated in Fig. 4. Near C^*, $g_{\mathrm{L}+}(\xi)$ $(\xi \sim d_- + d_+/2)$ as well as $g_{\mathrm{L}-}(0)$ exhibits an abrupt increase but $g_{\mathrm{L}+}(0)$ remains almost zero. This result is indicative that *the cations preferentially come into contact with the anions in contact with the surface*.

Similar plots for $d_+/d_{\mathrm{S}} = 1.80$ and $d_+/d_{\mathrm{S}} = 2.00$, respectively, are shown in Figs. 5 through 8. $H_{\mathrm{L}+}(0)$ and $H_{\mathrm{L}-}(0)$ simultaneously exhibit the divergent behavior at $C = C^*$. The simultaneous divergent behavior occurs at lower C^* as d_+ increases. The spinodal concentration C^* varies as follows: $C^* \sim 0.00825$ M and ~ 0.00258 M for $d_+/d_{\mathrm{S}} = 1.80$ and 2.00, respectively. Near C^*, $g_{\mathrm{L}+}(0)$ and $g_{\mathrm{L}-}(0)$ exhibit simultaneous,

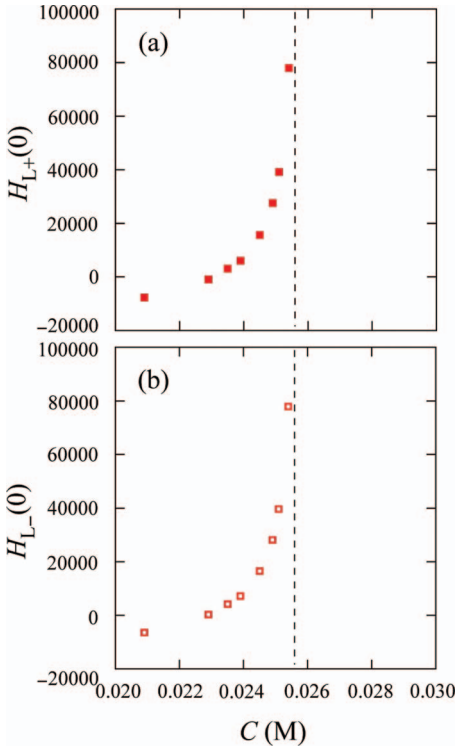

FIG. 3. (a) $H_{\mathrm{L}+}(0)$ plotted against C. (b) $H_{\mathrm{L}-}(0)$ plotted against C. C is the concentration of X_2PtCl_4 in the bulk, and $d_+/d_{\mathrm{S}} = 1.08$ (d_+ denotes the diameter of X^+). The definition of $H_{\mathrm{L}j}(0)$ $(j = +, -)$ is given by Eq. (4b). Beyond the spinodal concentration indicated by the broken line, the angle-dependent integral equation theory possesses no solutions.

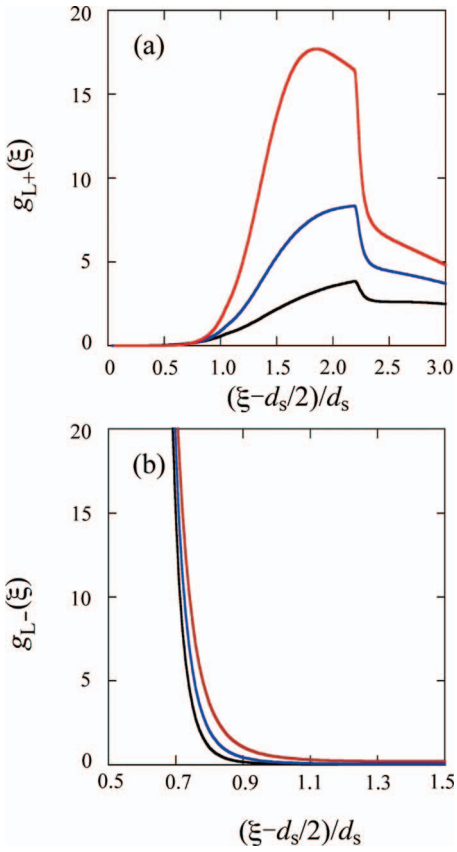

FIG. 4. Normalized density profiles of cations (a) and anions (b) in the vicinity of the surface ($g_{\mathrm{L}+}(\xi)$ and $g_{\mathrm{L}-}(\xi)$, respectively; ξ is the distance from the surface in the surface-normal direction). Black: $C = 0.0245$ M, blue: $C = 0.0251$ M, and red: $C = 0.0254$ M. C is the concentration of X_2PtCl_4 in the bulk, and $d_+/d_{\mathrm{S}} = 1.08$ (d_+ denotes the diameter of X^+). The contact values, $g_{\mathrm{L}+}(d_+/2)$, in the three bulk concentrations are all zero and the contact position is at $(\xi - d_{\mathrm{S}}/2)/d_{\mathrm{S}} = 0.04$. The contact values, $g_{\mathrm{L}-}(d_-/2)$ ($d_- = 2.16d_{\mathrm{S}}$ denotes the diameter of $[PtCl_4]^{2-}$), in the three bulk concentrations are 630.4, 1002, and 1606, respectively, and the contact position is at $(\xi - d_{\mathrm{S}}/2)/d_{\mathrm{S}} = 0.58$.

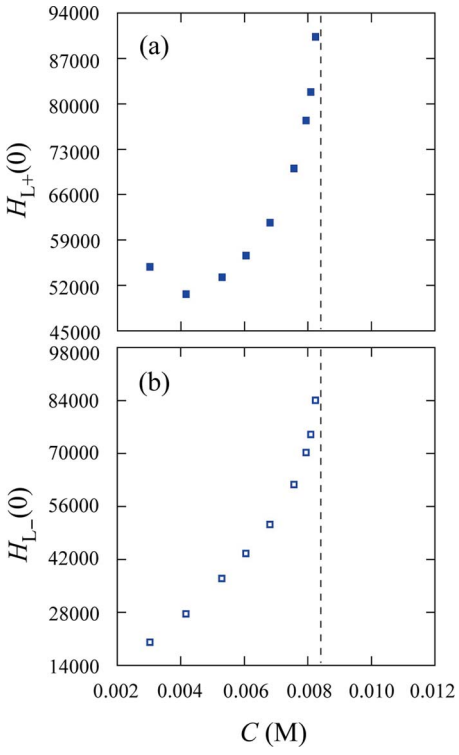

FIG. 5. (a) $H_{L+}(0)$ plotted against C. (b) H_{L-} (0) plotted against C. C is the concentration of X_2PtCl_4 in the bulk, and $d_+/d_S = 1.80$ (d_+ denotes the diameter of X^+). The definition of $H_{Lj}(0)$ ($j = +, -$) is given by Eq. (4b). Beyond the spinodal concentration indicated by the broken line, the angle-dependent integral equation theory possesses no solutions.

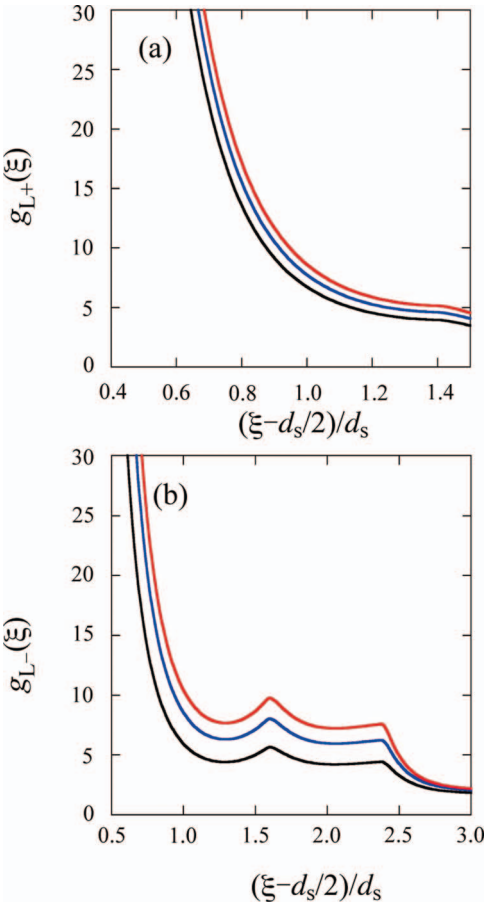

FIG. 6. Normalized density profiles of cations (a) and anions (b) in the vicinity of the surface ($g_{L+}(\xi)$ and $g_{L-}(\xi)$, respectively; ξ is the distance from the surface in the surface-normal direction). Black: $C = 0.00681$ M, blue: $C = 0.00794$ M, and red: $C = 0.00824$ M. C is the concentration of X_2PtCl_4 in the bulk, and $d_+/d_S = 1.80$ (d_+ denotes the diameter of X^+). The contact values, $g_{L+}(d_+/2)$, in the three bulk concentrations are 172.7, 194.2, and 212.7, respectively, and the contact position is at $(\xi - d_S/2)/d_S = 0.40$. The contact values, $g_{L-}(d_-/2)$ ($d_- = 2.16d_S$ denotes the diameter of $[PtCl_4]^{2-}$), in the three bulk concentrations are 36.56, 53.42, and 65.50, respectively, and the contact position is at $(\xi - d_S/2)/d_S = 0.58$.

abrupt increases. This result suggests that *the cations as well as the anions are in contact with the surface*.

We remark that cares must be taken in drawing Figs. 3, 5, and 7. Since the basic equations of the ADIET are solved not analytically but numerically, quite a robust numerical solution algorithm like ours is necessitated with very severe convergence criterion when C approaches C^*. The abrupt increases in $H_{L+}(0)$ and $H_{L-}(0)$ toward infinitely large values can then be traced out. As observed in the figures, it can be concluded that the ADIET possesses no solutions beyond C^* indicated by the broken line.

When the ADIET combined with the molecular model for water is employed, it is difficult to directly analyze the bridging transition because of the mathematical complexity. However, the analysis of the partial-wetting transition provides useful information on the bridging transition as well. We have investigated both of the two types of transitions in detail for the same system consisting of simple-liquid models, and the connection between them is rather straightforward. The pore diameter of our porous silicon is ∼3 nm on the average. The spinodal concentration for the bridging transition within such a narrow pore, C^{***}, should be considerably lower than C^*. The salt concentration at which the bridging transition actually occurs, C^{+++}, is even lower than C^{***}. The threshold value observed in our experiment for X^+ with $d_+/d_S = 1.08$, K^+, which is in the rage from 0.009 M to 0.010 M corresponds to C^{+++}. Thus, the theoretical results for X^+ with $d_+/d_S = 1.08$ are in agreement with the experimental observations in a semi-quantitative sense. This type of argument does not hold in the cases of X^+ with $d_+/d_S = 1.80$ and 2.00 as described in the first paragraph of Sec. V C.

V. COMPARISON BETWEEN EXPERIMENTAL AND THEORETICAL RESULTS

A. Real system treated in experiment

In the experiment, one of KCl, $(CH_3)_4NCl$, and $(C_2H_5)_4NCl$ is dissolved in water at the fixed concentration 0.5 M. K_2PtCl_4 is also dissolved and its concentration C in the bulk is gradually increased as an important parameter. The result manifests that the pores are abruptly filled with the second phase, in which the concentration of $[PtCl_4]^{2-}$ is remarkably enriched, at $C = C^{ex}$ (the superscript "ex" denotes "experimental"). The values of C^{ex} for KCl, $(CH_3)_3NCl$, and $(C_2H_5)_3NCl$ are, respectively, in the rages from 0.009 M to 0.010 M, from 0.007 M to 0.008 M, and from 0.006 M to 0.007 M.

As explained above, $(C_2H_5)_4N^+$ and $(CH_3)_4N^+$ are even more hydrophobic than $[PtCl_4]^{2-}$. $(C_2H_5)_4N^+$, for example, is smaller than $[PtCl_4]^{2-}$ but the former carries only the charge

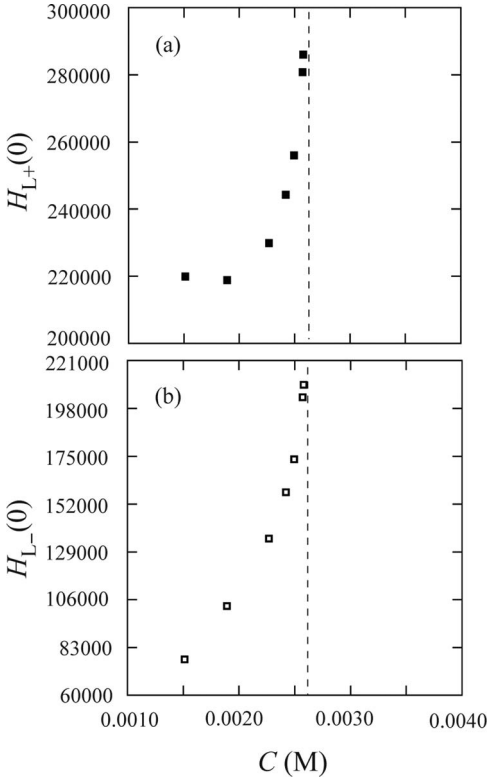

FIG. 7. (a) $H_{L+}(0)$ plotted against C. (b) $H_{L-}(0)$ plotted against C. C is the concentration of X_2PtCl_4 in the bulk, and $d_+/d_S = 2.00$ (d_+ denotes the diameter of X^+). The definition of $H_{Lj}(0)$ ($j = +, -$) is given by Eq. (4b). Beyond the spinodal concentration indicated by the broken line, the angle-dependent integral equation theory possesses no solutions.

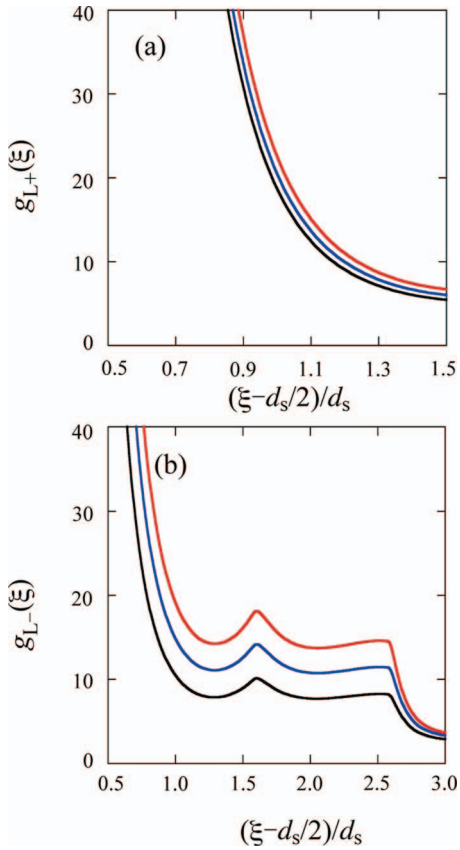

FIG. 8. Normalized density profiles of cations (a) and anions (b) in the vicinity of the surface ($g_{L+}(\xi)$ and $g_{L-}(\xi)$, respectively; ξ is the distance from the surface in the surface-normal direction). Black: $C = 0.00227$ M, blue: $C = 0.00250$ M, and red: $C = 0.00258$ M. C is the concentration of X_2PtCl_4 in the bulk, and $d_+/d_S = 2.00$ (d_+ denotes the diameter of X^+). The contact values, $g_{L+}(d_+/2)$, in the three bulk concentrations are 681.5, 739.3, and 805.3, respectively, and the contact position is at $(\xi - d_S/2)/d_S = 0.50$. The contact values, $g_{L-}(d_-/2)$ ($d_- = 2.16d_S$ denotes the diameter of $[PtCl_4]^{2-}$), in the three bulk concentrations are 57.07, 80.15, and 103.3, respectively, and the contact position is at $(\xi - d_S/2)/d_S = 0.58$.

e while the latter carries the charge $-2e$. Here, let us compare K_2PtCl_4 solution and $(CH_3)_4NCl$ solution. For each solution, only a single salt species is dissolved in water, and C denotes the concentration of K_2PtCl_4 or $(CH_3)_4NCl$ in the bulk. In K_2PtCl_4 solution, the theoretical result shows that the spinodal concentration for the partial-wetting transition $C^* \sim 0.0254$ M. Since $(CH_3)_4N^+$ is more hydrophobic than $[PtCl_4]^{2-}$, C^* in $(CH_3)_4NCl$ solution should be considerably lower than this value (both K^+ and Cl^- ions exhibit positive hydration, and these ions are not likely to affect C^*). C^{+++} in $(CH_3)_4NCl$ solution is further smaller. Therefore, the surface-induced phase transition occurs at the concentration of $(CH_3)_4NCl$ that is much lower than 0.5 M: At $C = 0.5$ M, the pores are filled with the second phase in which the concentration of $(C_2H_5)_4N^+$ is remarkably enriched. The surface-induced phase transition is accompanied by remarkable enrichment of Cl^-. When K_2PtCl_4 is added to the solution and its concentration is gradually increased, it is probable that the anions of Cl^- are *abruptly* replaced by those of $[PtCl_4]^{2-}$ at $C = C^{ex}$. Qualitatively the same argument can be made for $(C_2H_5)_4NCl$ solution because $(C_2H_5)_4N^+$ is more hydrophobic than $(CH_3)_4N^+$.

B. Model system considered in theoretical analysis

In the theoretical analysis, only a single salt species X_2PtCl_4 is dissolved in water and its concentration C in the bulk is gradually increased as an important parameter. It is observed that the partial wetting occurs for both X^+ and $[PtCl_4]^{2-}$. The values of the spinodal concentration C^* for X = K, $(CH_3)_4N$, and $(C_2H_5)_4N$ are, respectively, ~0.0254 M, ~0.00825 M, and ~0.00258 M. The partial wetting originates from the remarkable enrichment of the concentration of ions with large sizes (i.e., ions exhibiting negative hydration) near the hydrophobic surface. Namely, it is caused by only $[PtCl_4]^{2-}$ for X = K, whereas by the interplay of $[PtCl_4]^{2-}$ and $(CH_3)_4N^+$ or $(C_2H_5)_4N^+$ for X = $(CH_3)_4N$ or $(C_2H_5)_4N$. Even in the case of K_2PtCl_4, however, the partial wetting of $[PtCl_4]^{2-}$ is accompanied by that of K^+. It is probable that the partial wetting of $[PtCl_4]^{2-}$ alone would give rise to the energetic instability due to electrostatic repulsive interactions among the platinum complex anions. In general, the partial wetting of large cations or large anions is accompanied by that of ions carrying charges with the opposite sign irrespective of the ion size.

C. Information concerning cation-size effect

Because of the differences between the real and model systems described above, the experimental and theoretical

results cannot be compared quantitatively. Nevertheless, the following important point is demonstrated from both experimental and theoretical viewpoints: The surface-induced phase transition for an anion species with a large size is substantially influenced by a coexisting cation species with a large size; and the influence becomes stronger as the size of the cation species increases.

In the prevailing view based on classical electrochemistry, the anion concentration near the surface is normally determined by a balance of the electrochemical consumption and the supply by diffusion. The theory of electric double layer, in which the cation effect is taken into consideration only in terms of its ionic strength, is not capable of explaining the effect of cation species or cation size. Therefore, tuning an electrochemical reaction by the choice of the cation species coexisting with the anions is not common knowledge. By contrast, the present study shows that our theory based on statistical mechanics for confined molecular liquids is a powerful tool which enables us to reveal the microscopic mechanism of the effect of cation species. Such tuning is feasible, which has been demonstrated for a nanoporous electrode using the displacement deposition experiment and the statistical-mechanical theory for confined aqueous solutions combined with a molecular model for water.

VI. CONCLUDING REMARKS

We have investigated the effect of cation species (K^+, $(CH_3)_4N^+$, or $(C_2H_5)_4N^+$) coexisting with platinum complex anions ($[PtCl_4]^{2-}$) on electrochemical platinum deposition in nanoporous silicon. The pore diameter is ∼3 nm on the average and the pore wall surface is hydrophobic. Platinum complex (K_2PtCl_4) and one of the three salts, KCl, $(CH_3)_4NCl$, and $(C_2H_5)_4NCl$, are added to ultra pure water: Each of the resultant solutions is used for the platinum deposition bath. The concentration of K^+, $(CH_3)_4N^+$, or $(C_2H_5)_4N^+$ in the bulk is fixed at 0.5 M. The deposition experiment was performed by gradually increasing the concentration of $[PtCl_4]^{2-}$ in the bulk from 0.006 M with the increment of 0.001 M.

At a threshold concentration of $[PtCl_4]^{2-}$ in the bulk, the platinum deposition within nanopores is drastically accelerated with the result that a nanopore is densely packed with platinum nanoparticles. We find that the threshold concentration becomes lower as the cation size increases. The prevailing view based on classical electrochemistry is not capable of elucidating the observed effect of coexisting cations. The elucidation is made possible only by consulting a liquid-state theory based on statistical mechanics. In particular, it is crucial to employ a molecular model for water and treat confined aqueous solutions.

Our analysis using the angle-dependent integral equation theory[29,32–49] has suggested the following: The nanopores are abruptly filled with the second phase in which the ion concentration is orders of magnitude higher than that in the bulk; and not only the anions but also the cations are remarkably enriched in the second phase. This result, which was not noticed in our earlier work,[26] is not straightforward because the charge neutrality is not necessarily satisfied within the confined aqueous solution. Presumably, the remarkable enrichment of the anions alone would give rise to the energetic instability due to electrostatic repulsive interactions among the anions. The ions with large sizes, $[PtCl_4]^{2-}$, $(CH_3)_4N^+$, and $(C_2H_5)_4N^+$, are only weakly hydrated and excluded from the bulk to a hydrophobic surface. The threshold concentration is influenced only by a cation species possessing a sufficiently large size. Replacement of K^+ by Na^+, for example, would cause no change in the threshold concentration.

The present study provides important results from both scientific and practical viewpoints. It stimulates the researches in a new, very interesting field for liquid, liquid mixture, or aqueous solution confined in nanospace. More information is now available concerning the phase transition induced by a hydrophobic surface for aqueous electrolyte solutions containing only weakly hydrated ions. For further development of fuel cells, batteries, and capacitors in which nanoporous electrodes play essential roles, it may be an inevitable strategy to tune the behavior of electrochemical reaction for a particular ion species in solution using a coexisting ion species.

ACKNOWLEDGMENTS

This work was supported by JSPS Grant-in-Aid for Young Scientists (B) (No. 25810135: K. Fukami), by JSPS Grants-in-Aid for Scientific Research (B) (No. 25291035: M. Kinoshita), and by the Core Research for Evolutional Science and Technology (CREST) program of JST (K. Fukami and T. Abe). R. Koda is grateful for JSPS Research Fellowship (DC2).

[1]M. T. Alam, M. M. Islam, T. Okajima, and T. Ohsaka, J. Phys. Chem. C **112**, 16600 (2008).
[2]H. Föll, J. Carstensen, E. Ossei-Wusu, A. Cojocaru, E. Quiroga-Gonzalez, and G. Neumann, J. Electrochem. Soc. **158**, A580 (2011).
[3]M. Leisner, A. Cojocaru, E. Ossei-Wusu, J. Carstensen, and H. Föll, Nanoscale Res. Lett. **5**, 1502 (2010).
[4]R. Nakamura and H. Frei, J. Am. Chem. Soc. **128**, 10668 (2006).
[5]M. M. Orosco, C. Pacholski, and M. J. Sailor, Nat. Nanotechnol. **4**, 255 (2009).
[6]M. P. Schwartz, S. D. Alvarez, and M. J. Sailor, Anal. Chem. **79**, 327 (2007).
[7]Y. Yamauchi, A. Sugiyama, R. Morimoto, A. Takai, and K. Kuroda, Angew. Chem. Int. Ed. **47**, 5371 (2008).
[8]K. Fukami, M. L. Chourou, T. Sakka, and Y. H. Ogata, Phys. Status Solidi A **208**, 1407 (2011).
[9]K. Fukami, Y. Tanaka, M. L. Chourou, T. Sakka, and Y. H. Ogata, Electrochim. Acta **54**, 2197 (2009).
[10]F. Endres, N. Borisenko, S. Z. El Abedin, R. Hayes, and R. Atkin, Faraday Discuss. **154**, 221 (2012).
[11]M. Mezger, H. Schroder, H. Reichert, S. Schramm, J. S. Okasinski, S. Schoder, V. Honkimaki, M. Deutsch, B. M. Ocko, J. Ralston, M. Rohwerder, M. Stratmann, and H. Dosch, Science **322**, 424 (2008).
[12]N. Nishi, K. Kasuya, and T. Kakiuchi, J. Phys. Chem. C **116**, 5097 (2012).
[13]M. Rosa Castillo, J. M. Fraile, and J. A. Mayoral, Langmuir **28**, 11364 (2012).
[14]T. Ichii, M. Negami, M. Fujimura, K. Murase, and H. Sugimura, Electrochemistry **82**, 380 (2014).
[15]M. V. Fedorov and A. A. Kornyshev, Chem. Rev. **114**, 2978 (2014).
[16]M. V. Fedorov and R. M. Lynden-Bell, Phys. Chem. Chem. Phys. **14**, 2552 (2012).
[17]K. Kirchner, T. Kirchner, V. Ivanistsev, and M. V. Fedorov, Electrochim. Acta **110**, 762 (2013).
[18]R. M. Lynden-Bell, A. I. Frolov, and M. V. Fedorov, Phys. Chem. Chem. Phys. **14**, 2693 (2012).
[19]M. Kinoshita, Mol. Phys. **94**, 485 (1998).
[20]M. Kinoshita, Mol. Phys. **96**, 71 (1999).

[21]M. Kinoshita, Chem. Phys. Lett. **325**, 281 (2000).
[22]M. Kinoshita, Chem. Phys. Lett. **326**, 551 (2000).
[23]M. Kinoshita, Chem. Phys. Lett. **333**, 217 (2001).
[24]M. Kinoshita, "Surface-induced phase transition and long-range surface force: Roles in colloidal and biological systems," in *Recent Research Developments in Molecular Physics* (Transworld Research Network, India, 2003), Vol. 1, pp. 21–41, ISBN: 81-7895-113-4.
[25]K. Fukami, R. Koda, T. Sakka, T. Urata, K. Amano, H. Takaya, M. Nakamura, Y. Ogata, and M. Kinoshita, Chem. Phys. Lett. **542**, 99 (2012).
[26]K. Fukami, R. Koda, T. Sakka, Y. Ogata, and M. Kinoshita, J. Chem. Phys. **138**, 094702 (2013).
[27]Y. H. Ogata, K. Kobayashi, and M. Motoyama, Curr. Opin. Solid State Mater. Sci. **10**, 163 (2006).
[28]X. G. Zhang, *Electrochemistry of Silicon and its Oxide* (Springer, 2001).
[29]M. Kinoshita, J. Solution Chem. **33**, 661 (2004).
[30]H. Greberg and G. N. Patey,J. Chem. Phys. **114**, 7182 (2001).
[31]M. Mizukami, M. Moteki, and K. Kurihara, J. Am. Chem. Soc. **124**, 12889 (2002).
[32]P. G. Kusalik and G. N. Patey, J. Chem. Phys. **88**, 7715 (1988).
[33]P. G. Kusalik and G. N. Patey, Mol. Phys. **65**, 1105 (1988).
[34]G. M. Torrie, P. G. Kusalik, and G. N. Patey, J. Chem. Phys. **89**, 3285 (1988).
[35]G. M. Torrie, P. G. Kusalik, and G. N. Patey, J. Chem. Phys. **90**, 4513 (1989).
[36]G. M. Torrie, P. G. Kusalik, and G. N. Patey, J. Chem. Phys. **91**, 6367 (1989).
[37]G. M. Torrie and G. N. Patey, J. Phys. Chem. **97**, 12909 (1993).
[38]M. Kinoshita and M. Harada, Mol. Phys. **81**, 1473 (1994).
[39]M. Kinoshita, S. Iba, and M. Harada, J. Chem. Phys. **105**, 2487 (1996).
[40]M. Kinoshita and D. R. Bérard, J. Comput. Phys. **124**, 230 (1996).
[41]N. M. Cann and G. N. Patey, J. Chem. Phys. **106**, 8165 (1997).
[42]D. R. Bérard, M. Kinoshita, N. M. Cann, and G. N. Patey, J. Chem. Phys. **107**, 4719 (1997).
[43]M. Kinoshita, J. Mol. Liq. **119**, 47 (2005).
[44]M. Kinoshita, N. Matubayasi, Y. Harano, and M. Nakahara, J. Chem. Phys. **124**, 024512 (2006).
[45]M. Kinoshita, Condens. Matter Phys. **10**, 387 (2007).
[46]M. Kinoshita, J. Chem. Phys. **128**, 024507 (2008).
[47]M. Kinoshita and M. Suzuki, J. Chem. Phys. **130**, 014707 (2009).
[48]M. Kinoshita and T. Yoshidome, J. Chem. Phys. **130**, 144705 (2009).
[49]T. Yoshidome and M. Kinoshita, Phys. Chem. Chem. Phys. **14**, 14554 (2012).
[50]J. C. Shelley, G. N. Patey, D. R. Bérard, and G. M. Torrie, J. Chem. Phys. **107**, 2122 (1997).